The physics potential of HL-LHC

Editors:

Workshop steering group: A. Dainese, M.L. Mangano, A.B. Meyer, A. Nisati, G.P. Salam, M. Vesterinen
WG1 conveners: P. Azzi, S. Farry, P. Nason, A. Tricoli, and D. Zeppenfeld
WG2 conveners: M. Cepeda, S. Gori, P. Ilten, M. Kado, and F. Riva,
WG3 conveners: X. Cid-Vidal, M. D'Onofrio, P. J. Fox, R. Torre, and K. Ulmer
WG4 conveners: A. Cerri, V.V. Gligorov, S. Malvezzi, J. Martin Camalich, and J. Zupan
WG5 conveners: Z. Citron, J. F. Grosse-Oetringhaus, J. M. Jowett, Y.-J. Lee, U. Wiedemann, M. Winn
Contributing authors: see Addendum

ABSTRACT

This document presents the executive summary of the findings of the Workshop on "The physics of HL-LHC, and perspectives on HE-LHC", which has run for over a year since its kick-off meeting on 30 October – 1 November 2017. We discuss here the HL-LHC physics programme. As approved today, this covers *(a)* pp collisions at 14 TeV with an integrated luminosity of 3 ab^{-1} each for ATLAS and CMS, and 50 fb^{-1} for LHCb, and *(b)* Pb–Pb and p–Pb collisions with integrated luminosities of 13 nb^{-1} and 50 nb^{-1}, respectively. In view of possible further upgrades of LHCb and of the ions programme, the WG reports assume 300 fb^{-1} of luminosity delivered to an Upgrade II of LHCb, 1.2 pb^{-1} of integrated luminosity for p–Pb collisions, and the addition of collisions with other nuclear species. A separate submission covers the HE-LHC results.
The activity has been carried out by five working groups (WGs): "Standard Model" (WG1), "Higgs" (WG2), "Beyond the Standard Model" (WG3), "Flavour" (WG4) and "QCD matter at high density" (WG5). Their reports, extending this executive summary with more results and details, are available on the CERN Document Server [1–5], and will appear on arXiv. The WG results include both phenomenological studies and detailed simulations of the anticipated performance of the LHC detectors under HL-LHC conditions. These latter studies implement the knowledge acquired during the preparation of the technical design reports for the upgraded detectors, and reflect the experience gained by the experiments during the first two runs of the LHC. The documents describing in full detail the HL-LHC studies performed by the experiments can be found in Ref. [6] (available in early 2019) and in Ref. [7].
Three goals have been set for the Workshop: (i) to update and extend the projections for the precision and reach of the HL-LHC measurements, and for their interpretation; (ii) to highlight new opportunities for discovery of phenomena beyond the Standard Model (BSM), in view of the latest theoretical developments and of recent data; (iii) to explore possible new directions and/or extensions of the approved HL-LHC programme, particularly in the area of flavour, in the search for elusive BSM phenomena, and in the study of QCD matter at high density. In addition to enriching and consolidating the physics plans for HL-LHC, and highlighting the significant advances that the full HL-LHC programme will bring relative to today's landscape, this contribution to the European Strategy for Particle Physics Update process is intended to help put in perspective the physics potential of future projects beyond HL-LHC.

References

1. P. Azzi, S. Farry, P. Nason, A. Tricoli, and D. Zeppenfeld, (conveners), et al*, Standard Model Physics at the HL-LHC and HE-LHC* , CERN-LPCC-2018-03, CERN, Geneva, 2018. https://cds.cern.ch/record/2650160.
2. M. Cepeda, S. Gori, P. J. Ilten, M. Kado, and F. Riva, (conveners), et al*, Higgs Physics at the HL-LHC and HE-LHC*, CERN-LPCC-2018-04, CERN, Geneva, 2018. https://cds.cern.ch/record/2650162.
3. X. Cid-Vidal, M. D'Onofrio, P. J. Fox, R. Torre, and K. Ulmer, (conveners), et al*, Beyond the Standard Model Physics at the HL-LHC and HE-LHC*, CERN-LPCC-2018-05, CERN, Geneva, 2018. https://cds.cern.ch/record/2650173.
4. A. Cerri, V. V. Gligorov, S. Malvezzi, J. Martin Camalich, and J. Zupan, (conveners), et al*, Flavour Physics at the HL-LHC and HE-LHC*, CERN-LPCC-2018-06, CERN, Geneva, 2018. https://cds.cern.ch/record/2650175.
5. Z. Citron, A. Dainese, J. F. Grosse-Oetringhaus, J. M. Jowett, Y.-J. Lee, U. Wiedemann, and M. A. Winn, (conveners), et al*, Future physics opportunities for high-density QCD at the LHC with heavy-ion and proton beams*, CERN-LPCC-2018-07, CERN, Geneva, 2018. arXiv:1812.06772 [hep-ph]. https://cds.cern.ch/record/2650176.
6. The ATLAS and CMS Collaborations, *Report on the Physics at the HL-LHC and Perspectives for the HE-LHC*, CERN-LPCC-2019-01, CERN, Geneva, 2019. https://cds.cern.ch/record/2651134.
7. LHCb Collaboration, R. Aaij et al., *Physics case for an LHCb Upgrade II - Opportunities in flavour physics, and beyond, in the HL-LHC era*, arXiv:1808.08865.

1 Precision, exploration potential and breadth: the new frontiers of the HL-LHC physics programme

The analysis of LHC data since the time of the last European Strategy review (2012-2013) has confirmed the immense physics potential of the LHC to perform very precise and sensitive measurements, in spite of the highly challenging experimental environment, already now characterized by pile-up conditions well beyond those originally foreseen. Among others, examples of this are provided by the progress made in the exploration of the Higgs sector, where the coupling to electroweak (EW) gauge bosons and to all charged third-generation fermions have been established to better than 5 standard deviations (s.d.), by the measurement of Standard Model (SM) cross sections and distributions to the percent level (e.g. for the production of W and Z vector bosons), by the precise determination of the top quark and W boson mass, and by an ever growing set of studies in the flavour sector. The outstanding performance and versatility of the LHC experiments have also inspired a diverse research programme, ranging from precise measurements of total cross sections and forward physics, to the discovery of new families of hadrons, challenging the *status quo* of hadronic spectroscopy. In parallel, the progress of theoretical calculations has made it possible to sharpen the interpretation of the data, and to increase the sensitivity to potential deviations from the SM. Unexpected observations have also emerged from the study of collisions with heavy ions, questioning paradigms and opening new directions in the exploration of QCD matter at the highest densities.

The legacy of the last few years of LHC studies is therefore a stronger confidence in the LHC's potential to push the reach for precision and sensitivity well beyond what was originally assumed possible. The updated projections for key observables prepared by the WGs build on this coherent progress in reducing both theoretical and experimental systematic uncertainties, and in extending the scope of the programme to a broader range of measurements and probes of fundamental interactions.

These studies underscore the immense value provided, in all domains, by the HL-LHC era. The importance of collecting a dataset with large integrated luminosity has clearly emerged during the Workshop activities. It will give access to the rarest phenomena, and will be critical to reduce systematics or bypass their limitations with new analyses, leading to measurements of hitherto unanticipated precision. It will provide the relevant sensitivity to sectors of BSM phenomena that are still beyond the reach of current analyses, and ultimately it will allow us to get closer to answering the big open questions of our field. The selection of results presented here, and the more complete collection contained in the WG reports, define challenging new targets, and redesign the landscape of knowledge that will be available by the end of HL-LHC.

2 Higgs properties and EW phenomena

The determination of Higgs boson properties, and their connection to EW symmetry breaking (EWSB), is the primary target of the HL-LHC physics programme. Since 2012, the Higgs physics programme has rapidly expanded, with new ideas, more precise predictions and improved analyses, into a major program of precision measurements, as well as searches for rare production and decay processes. Outstanding opportunities have emerged for measurements of fundamental importance, such as the first direct constraints on the Higgs trilinear self-coupling and the natural width. The HL-LHC programme covers also searches for additional Higgs bosons in EWSB scenarios motivated by theories beyond the SM (BSM). Finally, a rigorous effective field theory (EFT) framework allows one to parametrise in a model independent way all EW and Higgs results. This section updates the key expectations for HL-LHC, and summarizes the interpretation of the future constraints on new physics in terms of EFT couplings. The complete set of results is available in Ref. [2]. This reappraisal of the future sensitivities relies on the Run 2 analyses improvements and assumes the detector performance targets established in the experiments' upgrade TDRs. Further improvements should be possible with analyses optimised for the HL-LHC data sets. The main Higgs boson measurement channels correspond to five production modes (the gluon fusion ggF, the vector boson fusion VBF, the associated production with a vector boson WH and ZH, and the associated production with a pair of top quarks ttH) and seven decay modes: $H \to \gamma\gamma$, ZZ^*, WW^*, $\tau^+\tau^-$, $b\bar{b}$, $\mu^+\mu^-$ and $Z\gamma$. The latter two decay channels, as yet unobserved, should become visible, in the SM, during the next two LHC runs. The rate measurements in the aforementioned production and decay channels yield measurements of the Higgs couplings in the so-called "κ-framework". This introduces a set of κ_i factors that linearly modify the coupling of the Higgs boson to SM elementary particles (i), including the effective couplings to gluons and photons, and assuming no additional BSM contribution to the Higgs total width, Γ_H. The projected uncertainties, combining ATLAS and CMS, are summarised in Fig. 1. They include today's theory uncertainties reduced by a factor of two, which is close to the uncertainty that would result from using the improved HL-LHC parton distribution functions (PDFs, see Section 4.1) and considering signal theory uncertainties as uncorrelated. Except for rare decays, the overall uncertainties will be dominated by the theoretical systematics, with a precision close to percent level.

The main Higgs boson couplings will be measured at HL-LHC with a precision at the percent level. Large statistics will particularly help the study of complex final states, such as those arising from ttH production. The constraining power of the current ttH analyses has been limited to plausible improvements in the theory predictions, in particular in the $H \to b\bar{b}$ channel. The 3.4% precision on κ_t thus obtained is mostly due to the other direct ttH measurement channels.

These coupling measurements assume the absence of sizable additional contributions to Γ_H. As recently suggested, the patterns of quantum interference between background and Higgs-mediated production of photon pairs or four leptons are sensitive to Γ_H. Measuring the off-shell four-fermion final states, and assuming the Higgs couplings to gluons and ZZ evolve off-shell as in the SM, the HL-LHC will extract Γ_H with a 20% precision at 68% CL. Furthermore, combining all Higgs channels, and with the sole assumption that the couplings to vector bosons are not larger than the SM ones ($\kappa_V \leq 1$), will constrain Γ_H with a 5% precision at 95% CL. Invisible Higgs boson decays will be searched for at HL-LHC in all production channels, VBF being the most sensitive. The combination of ATLAS and CMS Higgs boson coupling measurements will set an upper limit on the Higgs invisible branching ratio of 2.5%, at the 95% CL. The precision reach in the measurements of ratios will be at the percent level, with particularly interesting measurements of κ_γ/κ_Z, which serves as a probe of new physics entering the $H \to \gamma\gamma$ loop, can be measured with an uncertainty of 1.4%, and κ_t/κ_g, which serves as probe of new physics entering the $gg \to H$ loop, with a precision of 3.4%.

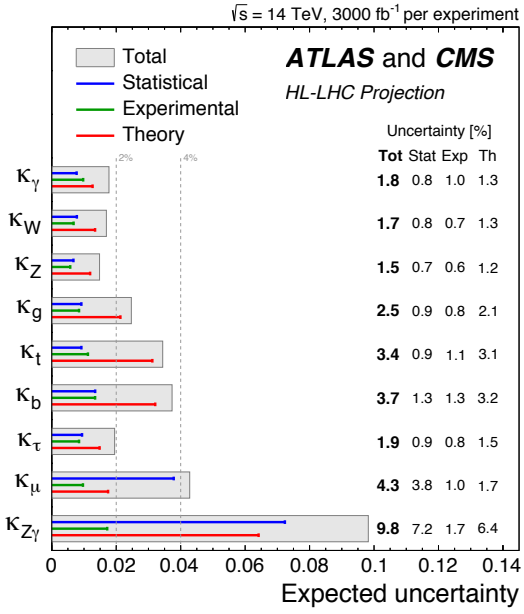

Figure 1. Projected uncertainties on κ_i, combining ATLAS and CMS: total (grey box), statistical (blue), experimental (green) and theory (red). From Ref. [2].

A summary of the limits obtained on first and second generation quarks from a variety of observables is given in Fig. 2 (left). It includes: (i) HL-LHC projections for *exclusive* decays of the Higgs into quarkonia; (ii) constraints from fits to differential cross sections of *kinematic* observables (in particular p_T); (iii) constraints on the total *width* Γ_H relying on different assumptions (the examples given in the Fig. 2 (left) correspond to a projected limit of 200 MeV on the total width from the mass shift from the interference in the diphoton channel between signal and continuous background and the constraint at 68% CL on the total width from off-shell couplings measurements of 20%); (iv) a *global* fit of Higgs production cross sections (yielding the constraint of 5% on the width mentioned herein); and (v) the *direct search* for Higgs decays to $c\bar{c}$ using inclusive charm tagging techniques. Assuming SM couplings, the latter is expected to lead to the most stringent upper limit of $\kappa_c \lessapprox 2$. A combination of ATLAS, CMS and LHCb results would further improve this constraint to $\kappa_c \lessapprox 1$.

The Run 2 experience in searches for Higgs pair production led to a reappraisal of the HL-LHC sensitivity, including several channels, some of which were not considered in previous projections: 2b2γ, 2b2τ, 4b, 2bWW, 2bZZ. Assuming the SM Higgs

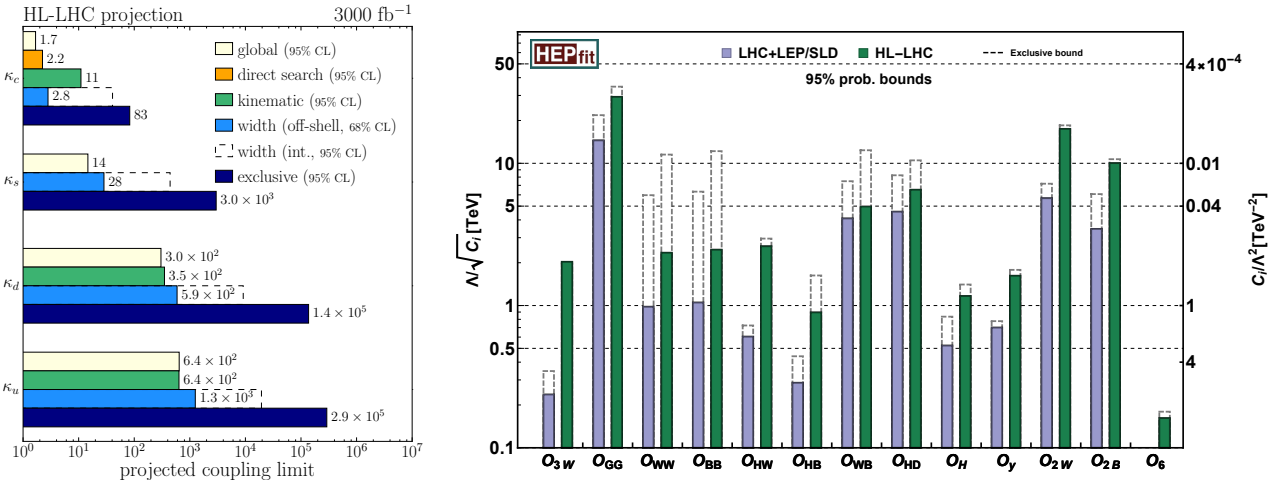

Figure 2. Left: Summary of the projected HL-LHC limits on the quark Yukawa couplings. Right: Summary of constraints on the SMEFT operators considered. The shaded bounds arise from a global fit of all operators, those assuming the existence of a single operator are labeled as "exclusive". From Ref. [2].

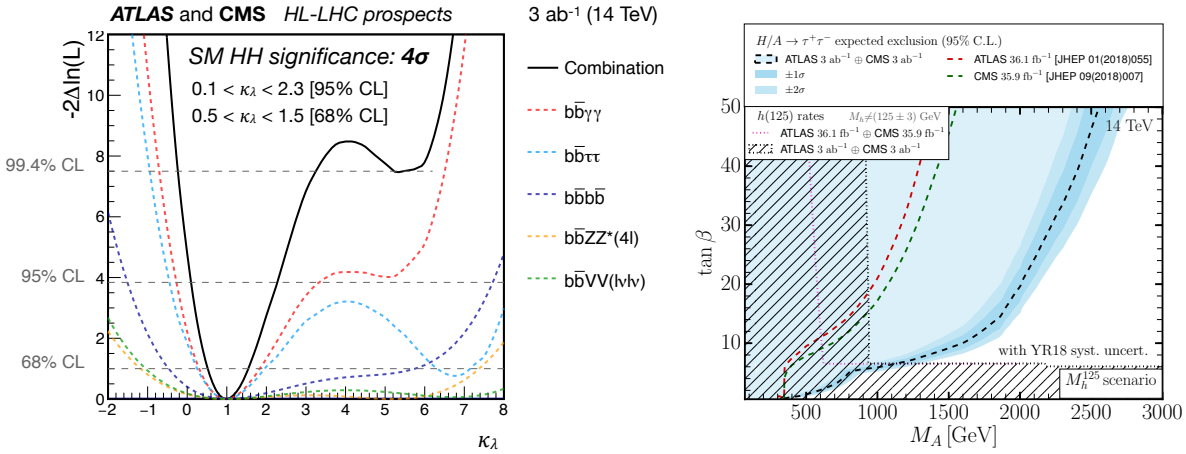

Figure 3. Left: Projected combined HL-LHC sensitivity to Higgs trilinear coupling from direct search channels. Right: sensitivity to BSM Higgs bosons, in the $H/A \to \tau\tau$ channel. From Ref. [2].

self-coupling λ, ATLAS and CMS project a sensitivity to the HH signal of approximately 3 s.d. per experiment, leading to a combined observation sensitivity of 4 s.d. These analyses, which make use also of the HH mass spectrum shape, result in the likelihood profile as a function of κ_λ shown in Fig. 3 (left). An important feature of these analyses is the presence of the secondary minimum in the likelihood lineshape, due to the degeneracy in the total number of HH signal events for different κ_λ values. We note that at the HL-LHC the secondary minimum can be excluded at 99.4% CL, with a constraint on the Higgs self-coupling of $0.5 < \kappa_\lambda < 1.5$ at the 68% CL. The results on HH production studies are statistics limited, therefore a dataset of at least 6 ab^{-1} (ATLAS and CMS combined) is essential to achieve this objective.

Higgs studies at HL-LHC will enhance the sensitivity to BSM physics, exploiting indirect probes via precision measurements, and a multitude of direct search targets, ranging from exotic decays of the 125 GeV Higgs boson (e.g. decays including light scalars, light dark photons or axion-like particles, and decays to long-lived BSM particles) to the production of new Higgs bosons, neutral and charged, at masses above or below 125 GeV. As an example, Fig. 3 (right) shows a summary of the MSSM regions of parameter space that will be probed by ATLAS and CMS. The expected exclusion limit for $H/A \to \tau\tau$ is presented in black-dashed and compared to the present limit (in red and green for ATLAS and CMS, respectively). The HL-LHC will have access to new Higgs bosons as heavy as 2.5 TeV for $\tan\beta > 50$. In the figure, we also present the expected bound coming from Higgs precision coupling measurements which excludes Higgs bosons with masses lower than approximately 1 TeV over a large range of $\tan\beta$.

Precision measurements provide an important tool to search for BSM physics associated to mass scales beyond the LHC direct reach. The EFT framework, where the SM Lagrangian is supplemented with dimension-6 operators $\sum_i c_i \mathcal{O}_i^{(6)}/\Lambda^2$, allows one to systematically parametrise BSM effects and how they modify SM processes. Figure 2 (right) shows the results of a global fit to observables in Higgs physics, as well as diboson and Drell-Yan processes at high energy. The fit includes all operators generated by new physics that only couples to SM bosons. These operators can either modify SM amplitudes, or generate new amplitudes. In the former case, the best LHC probes are, for example, precision measurements of Higgs branching ratios. In the case of the operator $\mathcal{O}_H$, for example, the constraints in Fig. 2 (right) translate into a sensitivity to the Higgs compositeness scale $f > 1.6$ TeV, corresponding to a new physics mass scale of 20 TeV for an underlying strongly coupled theory. The effects associated with some new amplitudes grow quadratically with the energy. For example, Drell-Yan production at large mass can access, via the operators $\mathcal{O}_{2W,2B}$, energy scales of order 12 TeV (Fig. 2).

2.1 Production of multiple EW gauge bosons

The measurement of production of pairs or triplets of EW gauge boson will be of great importance to test the mechanism of EW symmetry breaking, since it can signal the presence of anomalous EW couplings, and of new physics at energy scales beyond the reach of direct resonance production. First observations of EW multiboson interactions have recently been achieved in vector boson scattering (VBS) of WW and WZ and we expect a fuller picture to be accessible at HL-LHC, by statistics, but also through improved detector instrumentation and acceptance in the forward direction. Table 1 summarizes the expected SM yields, quoting the expected precision and significance for several HL-LHC measurements. In particular, the extraction of individual polarization contributions to same-sign WW scattering will yield a > 3 s.d. evidence for $W_L W_L$ production, combining ATLAS and CMS results.

Table 1. Expected precision and significance for the measurement of several EW multiboson processes [1].

Process	$W^{\pm}W^{\pm}$	WZ	WV	ZZ	WWW	WWZ	WZZ
Final state	$\ell^{\pm}\ell^{\pm}$jj	3ℓjj	ℓjjjj	4ℓjj	$3\ell3\nu$	$4\ell2\nu$	$5\ell\nu$
Precision	6%	6%	6.5%	10–40%	11%	27%	36%
Significance	$> 5\sigma$	$> 5\sigma$	$> 5\sigma$	$> 5\sigma$	$> 5\sigma$	3.0σ	3.0σ

2.2 $\sin^2\theta_{\text{eff}}$, m_W and m_{top}

The current world average of the weak mixing angle $\sin^2\theta_{\text{eff}} = 0.23153 \pm 0.00016$ is dominated by determinations based on data from LEP and from SLD. Those determinations, however, differ by over 3 s.d.. A precision extraction using HL-LHC data can help settle this long-standing issue, giving insight into the source of tension between LEP and SLD, whether this is the result of systematics, or of new physics. The statistical precision of $\sin^2\theta_{\text{eff}}$ measurements with ATLAS, CMS and LHCb will be better than $5 \cdot 10^{-5}$. The overall uncertainty will remain dominated by the PDFs, which can be reduced to $10-16 \cdot 10^{-5}$ using in situ constraints, with an overall uncertainty below $18 \cdot 10^{-5}$. The PDF uncertainty on $\sin^2\theta_{\text{eff}}$ can be reduced by $10\% - 25\%$ using the global fits to HL-LHC data, as discussed in Sec. 4.1. Data from the LHeC collider would have the potential to reduce the PDF uncertainties by an additional factor of 5.

Another key target of the LHC is to improve the knowledge of the W boson mass, m_W. The HL-LHC will greatly reduce the systematics, by limiting the PDF sensitivity via the extended leptonic coverage $|\eta| < 4$, and via its own PDF constraints. Dedicated low-pileup runs will provide the required conditions to optimize the reconstruction of missing transverse momentum, and five to ten weeks of data taking in the course of the HL-LHC will lead to a statistical precision of about 3 MeV. Experimental systematic uncertainties are largely of statistical nature, and with adequate efforts and exploiting the full available data sample, their impact can be maintained at a level similar to the statistical uncertainty. Assuming the extended lepton coverage allowed by the HL-LHC detectors, the impact of PDF uncertainties on the m_W measurement, using today's PDF sets, would amount to 5-8 MeV. These uncertainties are further reduced to about 4 MeV when using the HL-LHC ultimate PDF set (Sec. 4.1), leading to an overall HL-LHC target of $\Delta m_W = \pm 6$ MeV. LHeC measurements could further reduce the PDF systematics to 2 MeV.

The projections for the top mass measurements are collected in Table 2. With a mostly negligible statistical uncertainty, they reflect the anticipated measurement and modeling systematics, but do not include the uncertainty in the interpretation in terms of a theoretically well defined mass (see the discussion in Ref. [1]). Progress here will be driven by future theoretical developments, supported by the large amount of data and of probes of the top mass subject to independent theoretical systematics.

Table 2. Projected total uncertainties on the top quark mass, obtained with different methods. From Ref. [1].

Method:	$t\bar{t}$ lepton+jets	t-channel single top	$m_{SV\ell}$	J/ψ	$\sigma_{t\bar{t}}$
Δm_{top} (GeV):	0.17	0.45	0.62	0.50	1.2

3 Flavour physics

The LHCb experiment has demonstrated emphatically that the LHC is an ideal laboratory for a comprehensive programme of flavour physics. The LHCb Upgrade II, combined with the enhanced B-physics capabilities of the Phase II upgrades of ATLAS and CMS, will enable a wide range of flavour observables to be determined at HL-LHC with unprecedented precision, complementing and extending the reach of Belle II, and of the high-p_T physics programme. Some highlights are given here, see Ref. [4] for a comprehensive overview.

3.1 Testing CKM unitarity

The unitary nature of the CKM matrix, and the assumptions of the SM, impose nontrivial relations between the CKM elements, implying the closure of the vertices of the standard unitarity triangle, Fig. 4. The angle γ can be extracted with small experimental and theoretical systematics, but is the least well known ($\pm 5^\circ$), due to statistics. LHCb Upgrade II will improve the precision by an order of magnitude, or better. The precision measurement of the B_s weak mixing phase will be another highlight of the programme. The expected precision on $\phi_s^{c\bar{c}s}$ at the end of the HL-LHC period will be ~ 5 mrad for ATLAS and CMS, and ~ 3 mrad for LHCb . This will be at the same level as the current precision on the indirect determination based on the CKM fit using tree-level measurements. The anticipated impact of these improvements can be seen in Fig. 4. The increased sensitivity will allow for extremely precise tests of the CKM paradigm. In particular, it will permit the tree-level observables, which provide SM benchmarks, to be assessed against those with loop contributions, which are more susceptible to new physics.

3.2 Bottom quark probes of new physics and prospects for B-anomalies

The flavour-changing neutral current (FCNC) transitions $b \to s(d)\ell^+\ell^+$ provide some of the most sensitive probes of new physics. For most of the corresponding observables, this sensitivity is statistics limited. The HL-LHC, combining ATLAS, CMS and LHCb Upgrade II, is the only facility with the potential to distinguish between some plausible new physics scenarios. As an example, Fig. 5 shows the potential sensitivity to the C_9 and C_{10} Wilson coefficients, illustrating scenarios with modifications of just C_9 (vector current) and of both $C_9 = -C_{10}$ (pure left-handed current). The fits use the measurements of the branching

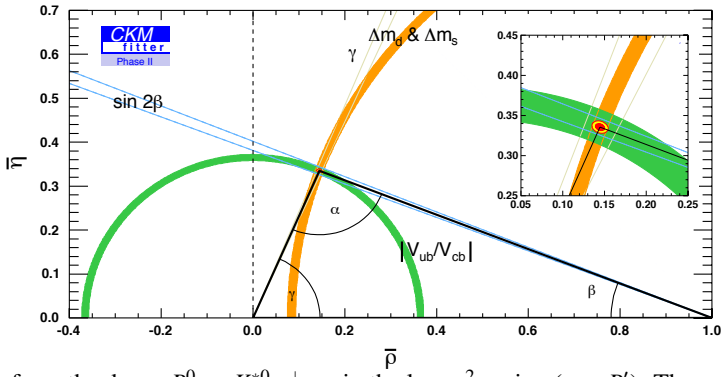

Figure 4. Projected constraints in the $\bar{\rho} - \bar{\eta}$ plane from LHCb measurements and lattice QCD calculations alone, after 300 fb^{-1} at the end of HL-LHC. From Ref. [4].

fraction $B_s \to \mu^+\mu^-$ and the angular observables from the decay $B^0 \to K^{*0}\mu^+\mu^-$ in the low-q^2 region (e.g. P_5'). The reach for generic new physics at tree-level is found to exceed 100 TeV, doubling the reach prior to the HL-LHC. An example of the impact of new physics on the ratio of branching fractions $\mathscr{B}(B_d \to \mu^+\mu^-)/\mathscr{B}(B_s \to \mu^+\mu^-)$ is shown on the right of Fig. 5, where a scatter plot of BSM models currently allowed by data is compared against the future 10% HL-LHC sensitivity.

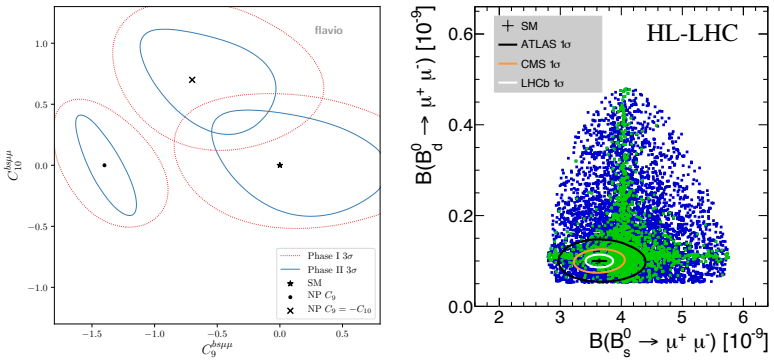

Figure 5. Left: Potential HL-LHC sensitivity to the Wilson coefficients C_9 (vector current) and $C_9 = -C_{10}$ (pure left-handed current), combining LHCb, ATLAS and CMS. Right: BR($B_s^0 \to \mu^+\mu^-$) vs. BR($B_d^0 \to \mu^+\mu^-$) in the SM (black mark), and in sets of BSM models with FCNC interactions consistent with current data (green points). The coloured contours show the expected 1 s.d. HL-LHC sensitivity of ATLAS, CMS, and LHCb Upgrade II. See Ref. [4] for details.

3.3 Top FCNC

The top quark is characterized by its large mass and its $\mathscr{O}(1)$ coupling to the Higgs, quite distinct from any other SM fermion. Studying top quark properties may shed light on the resolution of the SM flavour puzzle, or at least as to why one and only one Yukawa coupling is large. BSM models addressing the hierarchy problem may thus well leave an imprint in the top quark properties and decays. For instance, the top FCNCs, $t \to c\gamma, cZ, cg$ are null tests of the SM and are used as BSM probes. The search for these transitions is typically statistics limited, and will greatly benefit from the HL-LHC statistics. Current projections are shown in Table 3.

$t \to gu$	$t \to gc$	$t \to qZ$	$t \to \gamma u$	$t \to \gamma c$	$t \to Hq$
3.8×10^{-6}	3.2×10^{-5}	$2.4 - 5.8 \times 10^{-5}$	8.6×10^{-6}	7.4×10^{-5}	10^{-4}

Table 3. Projected reach for the 95% C.L. limits on the branching ratio for anomalous flavor changing top quark couplings [1].

3.4 Probing new physics with 2nd generation quarks and τ leptons

Indirect *CP* violation in the charm system is predicted to be very small in the SM, $\mathscr{O}(10^{-4})$ or less. In the absence of new physics contributions, the LHCb Upgrade II may well be the only facility with a realistic probability of observing it, reaching a sensitivity of $\mathscr{O}(10^{-5})$. A full programme of direct *CP*-violation searches in charm will also be performed, with complementary approaches and probing modes sensitive to both SM and new physics. Additionally, τ lepton decays offer a rich landscape to search for charged lepton flavour violation. The HL-LHC will be competitive with Belle-II in the $\tau \to \mu\mu\mu$ decay, with ATLAS, CMS and LHCb all approaching $\mathscr{O}(10^{-9})$ sensitivity on the branching ratio.

3.5 Hadron spectroscopy and QCD exotica

The LHC has had a transformative impact on the field of hadron spectroscopy, but this is only the beginning of a new era of measurements on the known states to determine their nature and opportunities for further particles to be observed. Due to its ability to reconstruct and analyze all collisions in real-time, LHCb Upgrade II will be able to collect a unique dataset for hadronic spectroscopy. This will enable a detailed and broad understanding of tetraquarks, pentaquarks, baryons containing multiple heavy quarks, and other yet-to-be-discovered exotic hadrons. While not directly sensitive to BSM effects, these measurements will play an important role in sharpening our understanding of QCD at the energy scales relevant for flavour physics, and hence make an important contribution to the accurate interpretation of any observed BSM anomalies.

4 QCD studies

4.1 PDF inputs

All hard production processes at the LHC start from a partonic collision, and their rate is determined by the PDFs. The knowledge of the PDFs is required to extract fundamental couplings from cross-section measurements (e.g. Higgs couplings from Higgs production rates), or from distributions (e.g. $\sin^2\theta_{\text{eff}}$ from forward-backward asymmetries in $Z^0 \to \ell^+\ell^-$). PDFs are also needed to predict the tails of SM distributions at large Q^2 (e.g. the jet p_T spectrum or the Drell-Yan (DY) mass distribution at large di-lepton mass), to probe the existence of new physics at high scales.

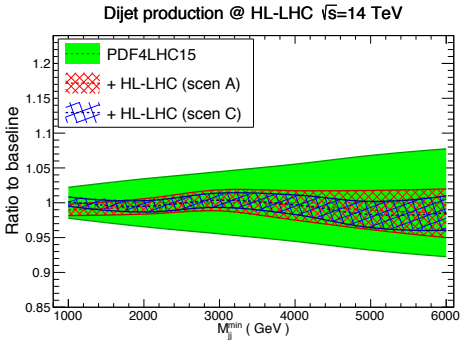

Figure 6. Reduction of the PDF uncertainty in the predicted cross section for jets. From Ref. [1].

Today's knowledge of PDFs will be improved at the HL-LHC by measuring a range of SM processes with jets, top quarks, photons and EW gauge bosons in the final state. The use of LHCb data, and access to large rapidities in ATLAS and CMS, will enhance the PDF sensitivity of these measurements. In the invariant mass region $M > 100$ GeV, the HL-LHC can improve the PDF uncertainties by a factor between 2 and 4, depending on the dominant partonic process and on the scenario for the systematic errors [1]. Two scenarios, A and C, were assumed, with a reduction by a factor of 2 and 5, respectively, of the experimental cross-section systematics relative to Run 2. These improvements will feed into improved theoretical predictions for a range of phenomenologically relevant processes both within and beyond the SM. As an example, Fig. 6 shows the impact of HL-LHC PDF data on the uncertainties for dijet production rates. For the $gg \to H$ process, the PDF systematics will be reduced to below 2%. More examples of the impact of these "ultimate" HL-LHC PDFs are discussed in Sect. 2.2. We also notice that high precision of cross-section measurements rely on further improvements in the determination of the integrated luminosity. For the HL-LHC, high precision luminosity detectors are currently being designed. Refined analysis techniques for the van der Meer scans, and novel approaches, such as the measurement of fiducial Z^0 boson production rates exploiting in-situ efficiency determination, can lead to further advances towards the percent level.

4.2 High-Q^2 processes

Studies of jet production at HL-LHC show that the experimental uncertainty on the cross-section measurements in the jet p_T range of 0.1–3 TeV, dominated by the jet energy scale, can be reduced to a $2.5-5\%$ level. This is a factor of 2 improvement with respect to Run 2 data, thanks to the large statistics available from data for the calibration at high p_T. Inclusive jet and di-jet samples in a central rapidity range will respectively extend the reach in jet p_T from 3.5 TeV in Run-2 up to about 5 TeV, and the dijet invariant mass (m_{jj}) from 9 TeV in Run-2 up to about 11 TeV.

Similar studies for inclusive production of isolated-photons (in association with a jet) show an extension of the kinematic reach from 1.5 TeV ($m_{\gamma-jet} = 3.3$ TeV) in Run-2 to about $E_T = 3.5$ TeV ($m_{\gamma-jet} = 7$ TeV). Measurements of jet and photon production at the HL-LHC will therefore probe QCD perturbation theory at unprecedented energy scales. The combined reduction in experimental, theoretical and PDF systematics will also significantly increase the sensitivity to possible new physics.

5 Searches for new physics at high mass

The HL-LHC will offer new possibilities to test many BSM scenarios, motivated by long-standing problems such as EW naturalness, dark matter (DM), the flavour problem, neutrino masses, the strong CP problem, and baryogenesis. All these new physics manifestations predict the existence of new particles, which can be searched for at HL-LHC profiting from the much larger statistics, slightly higher energy (14 TeV), and upgraded detectors. We highlight a subset of key results, selected among a large number of studies for different new physics scenarios [4]. All quoted exclusion (discovery) reaches refer to 95% CL (5σ).

5.1 Supersymmetry

The extension of the kinematic reach for supersymmetry (SUSY) searches at the HL-LHC is reflected foremost in the sensitivity to EW states, including sleptons, but also for gluinos and squarks. Studies under various hypothesis were made [3], including prompt and long-lived SUSY particle decays. Wino-like ($\tilde{w}$) chargino pair production processes are studied considering dilepton final states. Masses up to 840 (660) GeV can be excluded (discovered) for charginos decaying as $\tilde{\chi}_1^{\pm} \to W^{(*)}\tilde{\chi}_1^0$, in R-parity conserving scenarios with $\tilde{\chi}_1^0$ as the lightest supersymmetric particle (LSP). The results extend the mass reach obtained with 80 fb^{-1} of 13 TeV pp collisions by about 500 GeV, and extend beyond the LEP limit by almost an order of magnitude. Compressed SUSY spectra are theoretically well motivated but are among the most challenging scenarios experimentally, and

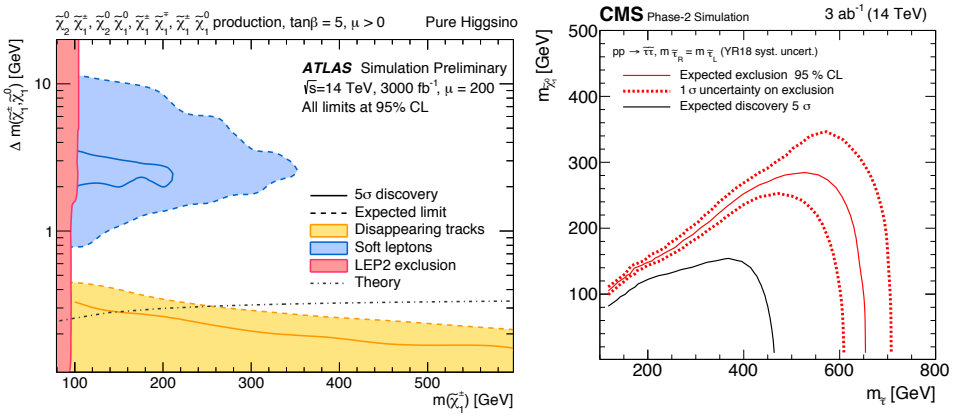

Figure 7. Left: Expected exclusion/discovery reach from the disappearing track (yellow) and dilepton (blue) searches in the $(\Delta m(\tilde{\chi}_1^\pm,\tilde{\chi}_1^0), m(\tilde{\chi}_1^\pm))$ mass plane. Right: Exclusion/discovery contours for $\tilde{\tau}$ pair production in the $(m_{\tilde{\tau}}, m_{\tilde{\chi}_1^0})$ mass plane. From Ref. [3].

are barely covered by the Run 2 analyses. HL-LHC searches for low momentum leptons will be sensitive to $\tilde{\chi}^\pm$ masses up to 350 GeV for $\Delta m(\tilde{\chi}_1^\pm,\tilde{\chi}_1^0) \approx 5$ GeV, and to mass splittings between 0.8 and 50 GeV, thus bringing significant new reach to higgsino ($\tilde{h}$) models. Similar search techniques can also be used to target pair produced $\tilde{e}$ and $\tilde{\mu}$ in compressed scenarios. If $\Delta m(\tilde{\chi}_1^\pm,\tilde{\chi}_1^0) < 1$ GeV, charginos can decay after the inner layers of the pixel detectors. Results for prompt (one of the analyses) and long-lived charginos (see below) are shown in Fig. 7 (left).

Dedicated searches for sleptons, characterised by the presence of at least one hadronically-decaying τ and missing E_T, will be sensitive to *currently unconstrained* pair-produced $\tilde{\tau}$: exclusion (discovery) for $m_{\tilde{\tau}}$ up to around 700 (500) GeV can be achieved under realistic assumptions of performance and systematic uncertainties, as shown in Fig. 7 (right).

In the strong SUSY sector, HL-LHC will probe gluino masses up to 3.2 TeV, with discovery reach around 3 TeV, in R-parity conserving scenarios and under a variety of assumptions on the $\tilde{g}$ prompt decay mode. This is about 0.8-1.0 TeV beyond the Run 2 $\tilde{g}$ mass reach for 80 fb^{-1}. Pair-production of top squarks ($\tilde{t}_1$) has been studied assuming $\tilde{t}_1 \to t\tilde{\chi}_1^0$ and fully hadronic final states with large missing E_T. Top squarks can be discovered (excluded) up to masses of 1.25 (1.7) TeV for $m\left(\tilde{\chi}_1^0\right) \sim 0$, i.e. $\Delta m(\tilde{t}_1,\tilde{\chi}_1^0) \gg m_t$, under realistic uncertainty assumptions. This extends by about 700 GeV the reach of Run 2 for 80 fb^{-1}. The reach in $m_{\tilde{t}}$ degrades for larger $\tilde{\chi}_1^0$ masses. If $\Delta m(\tilde{t}_1,\tilde{\chi}_1^0) \sim m_t$, the discovery (exclusion) reach is 650 (850) GeV.

5.2 Dark Matter and Dark Sectors

Compressed SUSY scenarios, as well as other DM models, can be targeted using signatures such as mono-jet, mono-photon and vector-boson-fusion (VBF) production. Mono-photon and VBF events allow targeting an EW fermionic triplet (minimal DM), equivalent to a wino-like signature in SUSY, for which there is no sensitivity in Run 2 searches with 36 fb^{-1}. Masses of the $\tilde{\chi}_1^0$ up to 310 GeV (130 GeV) can be excluded by the mono-photon (VBF) channel, with improvements possible if theoretical uncertainties are reduced. Projections for searches for a mono-Z signature, with $Z \to \ell^+\ell^-$ recoiling against missing E_T, have been interpreted in terms of models with a spin-1 mediator, and models with two Higgs doublets and an additional pseudo-scalar mediator a coupling to DM (2HDMa). The exclusion is expected for mediator masses up to 1.5 TeV, and for DM and pseudo-scalar masses up to 600 GeV, a factor of ~ 3 better than the 36 fb^{-1} Run-2 constraints. The case of 2HDMa models is complemented by 4-top final states, searched for in events with two same-charge leptons, or with at least three leptons. While searches using 36 fb^{-1} Run 2 data have limited sensitivity considering the most favourable signal scenarios (e.g. $\tan\beta = 0.5$), HL-LHC will probe possible evidence of a signal with $\tan\beta = 1$, $m_H = 600$ GeV and mixing angle of $\sin\theta = 0.35$, assuming m_a masses between 400 GeV and 1 TeV, and will allow exclusion for all 200 GeV $< m_a <$ 1 TeV. For DM produced in association with bottom or top quarks, where a (pseudo)scalar mediator decays to a DM pair, the HL-LHC will improve the sensitivity to mediator masses by a factor of 3-8 relative to the Run 2 searches with 36 fb^{-1}.

A very interesting scenario in the search for portals between the visible and dark sectors is that of the dark photon A'. As shown in Fig. 8, prospects for an inclusive search for dark photons decaying into muon or electron pairs indicate that the HL-LHC could cover a large fraction of the theoretically favored $\varepsilon - m_{A'}$ parameter space, where ε is the kinetic mixing between the photon and the dark photon and $m_{A'}$ the dark photon mass.

5.3 Resonances

Studies of resonance searches have been performed in a variety of final states and are documented in Ref. [3]. A sample of these results is presented here. A right-handed gauge boson with SM couplings, decaying as $W_R \to bt(\to b\ell\nu)$, can be excluded (discovered) for masses up to 4.9 (4.3) TeV, 1.8 TeV larger than the 36 fb^{-1} Run 2 result. For a sequential SM (SSM) W' boson in $\ell\nu$ final states ($\ell = e,\mu$), the mass reach improves by more than 2 TeV w.r.t. the Run 2 (80 fb^{-1}) reach, and by more than 1 TeV w.r.t. 300 fb^{-1}. The HL-LHC bound will be $M_{W'} > 7.9$ TeV, with discovery potential up to 7.7 TeV. Projections for

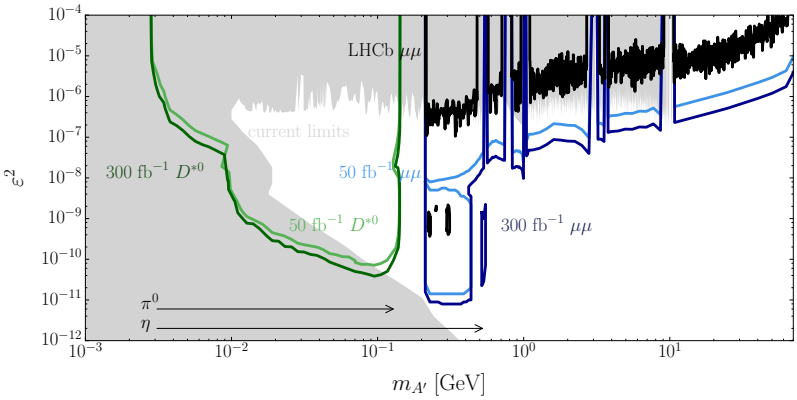

Figure 8. Current limits (grey), current LHCb limits (black band), and proposed future experimental reach (coloured bands) on A' parameter space. The arrows indicate the available mass range from light meson decays into $e^+e^-\gamma$. From Ref. [3].

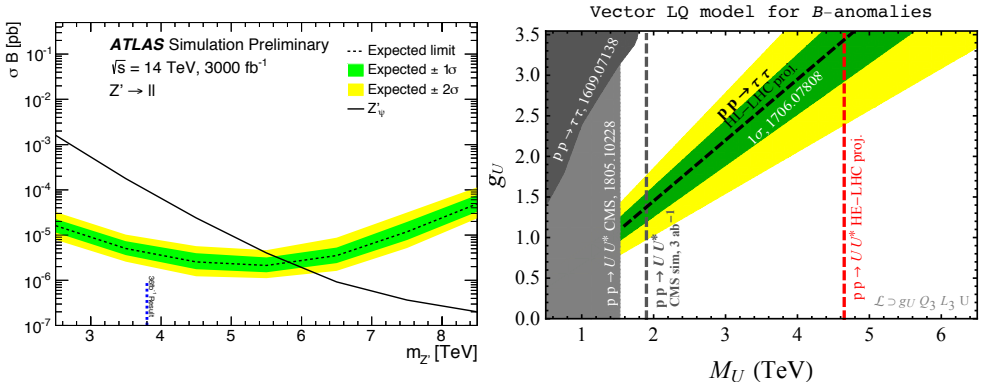

Figure 9. (Left) Expected (dashed black line) upper limit on cross section times branching fraction $\sigma \times \mathscr{B}$ as a function of the Z' boson mass. (Right) Projected sensitivity to a vector leptoquark model addressing the B decay anomalies. From Ref. [3].

searches for the SSM and E_6 Z' bosons, $Z'_{\rm SSM}$ and Z'_{ψ}, in the dilepton final state predict exclusion (discovery) up to masses of 6.5 TeV (6.4 TeV) and 5.8 TeV (5.7 TeV), respectively. The 36 fb^{-1} Run-2 exclusion for $Z'_{\rm SSM}$ (Z_{ψ}) is 4.5 TeV (3.8 TeV), expected to grow to 5.4 TeV (4.8 TeV) after 300 fb^{-1} (Fig. 9). Using top-tagging, a Randall–Sundrum Kaluza–Klein gluon decaying to $t\bar{t}$ is expected to be excluded (discovered) up to 6.6 TeV (5.7 TeV) extending the 36 fb^{-1} bounds by over 2 TeV.

Models related to the apparent flavour anomalies in B decays suggest the presence of heavy resonances, either Z' or leptoquarks (LQ), coupling to second and/or third generation SM fermions. The HL-LHC will be able to cover a significant portion of the parameter space allowed by flavor constraints, with an exclusion reach up to 4 TeV for the Z', depending on the structure and size of the Z' couplings. Pair produced scalar LQs coupling to μ (τ) and b-quarks, on the other hand, can be excluded up to masses of 2.5 (1.5) TeV, depending on assumptions on couplings. In Fig. 9 (right) we show the parameter space of a vector LQ model addressing B decay flavor anomalies (see Section 3.2) that can be covered with dedicated HL-LHC high-p_T searches. Finally, prospect studies for third generation LQ in the $t\mu$ and $t\tau$ channels deliver mass limits (discovery potential) increased by 500 (400) GeV with respect to 36 fb^{-1}, with discovery prospects in the $t\mu$ channel up to 1.7 TeV.

5.4 Long-lived particles

In addition to the significant expansion of expected luminosity, new detector upgrades will enable searches in the long-lived particle regime. Muons displaced from the beamline, such as found in SUSY models with $\tilde{\mu}$ lifetimes of $c\tau > 25$ cm, can be excluded at 95% CL. New fast timing detectors will also be sensitive to displaced photon signatures arising from long lived particles in the $0.1 < c\tau < 300$ cm range.

Prospect studies for disappearing tracks searches using simplified models of $\tilde{\chi}^{\pm}$ production lead to exclusions of chargino masses up to m($\tilde{\chi}_1^{\pm}$) = 750 GeV (1100 GeV) for lifetimes of 1 ns for the $\tilde{h}$ ($\tilde{w}$) hypothesis. When considering the lifetime predicted by theory, $\tilde{h}$ ($\tilde{w}$) masses up to 300 (830) GeV can be excluded. This improves the 36 fb^{-1} Run 2 mass reach by a factor of 2-3. The discovery reach is reduced to 160 GeV ($\tilde{h}$) and 500 GeV ($\tilde{w}$), due to the loss in acceptance at low lifetime (0.2 ns), but sensitivity is expected to be recovered with dedicated optimisations. Results are shown in Fig. 7 (left).

Several studies are available also for long-lived $\tilde{g}$. As an example, we expect a 1 TeV extension of the 36 fb^{-1} Run 2 mass reach, for models with $\tilde{g}$ lifetimes $\tau > 0.1$ ns, and an exclusion of $m_{\tilde{g}}$ up to 3.4-3.5 TeV. Finally, the signature of long-lived dark photons decaying to displaced muons can be reconstructed with dedicated algorithms and is sensitive to very small coupling $\varepsilon^2 \sim 10^{-14}$ for masses of the dark photons between 10 and 35 GeV. Complementarities in long-lived particle searches and enhancements in sensitivity might be achieved if new proposals for detectors and experiments such as Mathusla, FASER, Codex-B, MilliQan and LHeC are realized in parallel to the HL-LHC.

6 Forward Physics

Central exclusive production (CEP) corresponds to the production of a central system X, and nothing else, with two outgoing intact protons: $pp \to p + X + p$. Such a process may be mediated by photon exchange, with the elastic photon emission vertex leaving the protons intact. A range of SM (e.g. $X = \gamma\gamma$, $Z\gamma$, ZZ, $\ell\bar{\ell}$) and BSM states (e.g. $X =$ axion–like particles, monopoles, SUSY particles) may be produced in this way. CEP therefore allows one to use the LHC as a high-energy $\gamma\gamma$ collider, operating in a clean and well understood environment. These processes, in particular at higher mass, have small cross sections, and their detection requires taking data during the during standard LHC runs, with tagged protons. The HL-LHC statistics will make it possible to extend the sensitivity to higher masses and lower cross sections, increasing the discovery potential. New physics manifestations can be described by an effective Lagrangian with high-dimension operators. Among these operators, pure photon dimension-eight operators in the $\gamma\gamma\gamma\gamma$ interaction can be probed in $pp \to p(\gamma\gamma \to \gamma\gamma)p$ reactions. With proton tagging, one can probe $\gamma\gamma \to \gamma\gamma$ collisions, with the invariant mass of the $\gamma\gamma$ system ranging from about 300 GeV to 2 TeV. The expected bounds on the most sensitive anomalous couplings will be reduced by a factor of 5 at the HL-LHC compared to 300 fb^{-1}, without using time-of-flight information, and can be further improved by 20% with a 10 ps time-of-flight resolution. Similarly, at the HL-LHC we can study the anomalous $\gamma\gamma \to \gamma Z$ scattering that can be probed in $pp \to p(\gamma\gamma \to \gamma Z)p$ reactions. The sensitivity on the best probed anomalous coupling can be reduced by a factor of 10 compared to 300 fb^{-1}. The time-of-flight measurement can further improve the expected bounds by a factor of ~ 2 .

7 High-density QCD with heavy-ion and proton beams

Experiments with heavy-ion collisions at the LHC study strongly-interacting matter ("QCD matter") under the most extreme conditions of density and temperature accessible in the laboratory. The main focus at the LHC is learning how collective phenomena and macroscopic properties, involving many degrees of freedom, emerge from strong-interaction physics in the non-perturbative regime at the microscopic (quark, gluon) level. The high-luminosity heavy-ion programme starts in Run 3, when the peak Pb–Pb luminosity will be $\sim 10\times$ the original LHC design value. The integrated luminosity target of 13 nb^{-1} by the end of Run 4 represents a seven-fold increase with respect to Run 2. This programme offers the unique opportunity to investigate high-density QCD and the Quark-Gluon Plasma (QGP) towards four main goals:

1. Characterizing the macroscopic long-wavelength properties of the QGP with unprecedented precision.
2. Accessing the microscopic parton dynamics underlying QGP properties.
3. Developing a unified picture of QCD particle production from small (pp) to larger (pA and AA) systems.
4. Probing nuclear PDFs in a broad (x, Q^2) range, searching for the possible onset of parton saturation.

Each goal comprises a large set of new or highly-improved measurements, enabled by the detector upgrades of the four experiments, and requiring the updated programme (systems and luminosity targets) outlined at the end of the section. At the same time, a strong collaboration between theoretical and experimental groups leading to a sustained development on theory and modelling is crucial for achieving these goals. A subset of these measurements is described in the following.

Macroscopic properties of the QGP. It is by now well established that the long-wavelength behaviour of hot and dense QCD matter can be described in terms of fluid- and thermo-dynamic concepts. This behaviour is experimentally investigated using measurements of low-momentum (< 5 GeV/c) hadron production and flow patterns, as well as of electromagnetic radiation. Among the macroscopic properties of the QGP that will strongly benefit from the large luminosity increase, the temperature will be, for the first time at the LHC, determined with an accuracy of about 20% by measuring thermal radiation. Another notable example is the heavy-quark diffusion coefficient $2\pi T D_s$, which at a temperature T of 1–2$\times$ the QCD critical temperature T_c will be constrained with a 2$\times$ improved accuracy, as shown in Fig. 10, using measurements of the production and flow of several charm meson and baryon species.

Microscopic structure and inner workings of the QGP. For the first time the nature of the effective constituents of QCD matter and its characteristic length scales can be studied experimentally with high precision. Hard processes provide us with probes that should resolve the scale of the constituents and test its inner workings, that is the microscopic-level (point-like) interactions. Multi-differential jet measurements are one of the main avenues for these investigations. These include the Z–jet recoil measurements with 4$\times$ reduced uncertainties (see Fig. 11-left) and novel jet-substructure studies that are sensitive to the details of energy-loss mechanisms and to the medium degrees of freedom at small length scales. The aforementioned heavy-quark diffusion studies probe instead the degrees of freedom at larger length scales. Measurements of the production of charmonium and bottomonium states with different binding energies give access to a well-defined set of length scales for the study of the QCD potential and its modification in a colour-deconfined medium via the characterization of the mechanisms of melting and regeneration.

QCD dynamics from small to larger systems. Recent discoveries of collective patterns and strangeness content in particle production in pp and p–Pb collisions question both the view of pp collisions as a superposition of quasi-independent parton–parton scatterings and the view of nucleus–nucleus (large volume) collisions as a required precondition for a hydrodynamic

and opaque medium to form. High-precision studies of rare probes in small systems motivate an extension of the original programme, to address outstanding open questions on the existence of a medium in these collisions and on the possible formulation of a common picture of QCD multi-particle dynamics across all collision systems. Example studies that require very large integrated luminosity in both high-multiplicity pp and p–Pb collisions include the comparison of heavy-quark and quarkonium flow in small and large systems (see Fig. 11-middle) and the searches for thermal radiation and partonic energy loss (see Fig. 11-right, using hadron-jet recoil to search for a shift in jet momentum). The latter is an outstanding puzzle because the observed collective patterns require final-state interactions that should also lead to energy loss. The study of pp, p–Pb as well as O–O collisions promises to solve this puzzle.

Nuclear parton densities and search for saturation. High-luminosity p–Pb and Pb–Pb runs, which also produce γ–Pb collisions, will provide highly-improved precision and kinematic coverage for measurements of the PDFs in nuclei, from the high-Q^2 and $x \sim 10^{-3}$–10^{-1} region, with Z, W, dijets, and top quarks, down to the presently-uncovered small-x region below 10^{-4} with forward Drell-Yan and photons, where non-linear QCD evolution and parton phase-space saturation could set in. For example, W asymmetry measurements as a function of rapidity in p–Pb collisions are expected to reduce by 3–4$\times$ the uncertainty on the modification of the gluon PDF at $x = 10^{-2}$ and $Q^2 = 100\,\mathrm{GeV}^2$. These studies, besides their intrinsic interest, are crucial inputs for the initial conditions of heavy-ion collisions and they contribute to motivating the proposal for an extension of the p–Pb programme.

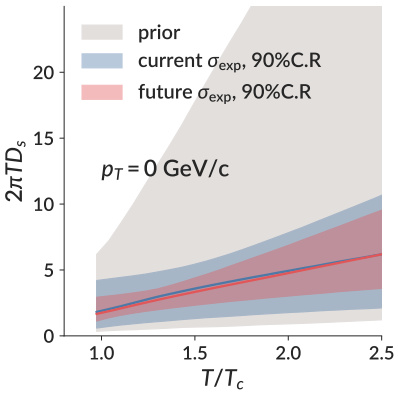

Figure 10. Charm diffusion coefficient as a function of temperature relative to the critical temperature T_c (ALICE and CMS combined) [5].

To accomplish this physics programme, the following colliding systems and luminosities are proposed.

- Pb–Pb ($A = 208$) at $\sqrt{s_{\mathrm{NN}}} = 5.5\,\mathrm{TeV}$ (research goals 1 and 2): $L_{\mathrm{int}} = 13\,\mathrm{nb}^{-1}$ and pp reference at the same energy
- p–Pb at $\sqrt{s_{\mathrm{NN}}} = 8.8\,\mathrm{TeV}$ (research goals 3 and 4): $1.2\,\mathrm{pb}^{-1}$ ATLAS/CMS, $0.6\,\mathrm{pb}^{-1}$ ALICE/LHCb, and pp reference
- pp at $\sqrt{s} = 14\,\mathrm{TeV}$ (research goal 3): $200\,\mathrm{pb}^{-1}$ in low-pileup conditions allows one to study extreme multiplicity events as large as 15$\times$ the average multiplicity, being equivalent to mid-peripheral (60–65% centrality) Pb–Pb collisions
- O–O ($A = 16$) at $\sqrt{s_{\mathrm{NN}}} = 7\,\mathrm{TeV}$ (research goal 3): a one week period, also accommodating a short p–O run to provide crucial input for cosmic-ray particle production models

Furthermore, it is pointed out that collisions of lighter ions, e.g. Ar–Ar ($A = 40$), represent an interesting case for extending the heavy-ion programme in Run 5. This would enable a $> 10\times$ increase of the nucleon–nucleon luminosity, giving access to novel observables in the sectors of hard and electromagnetic probes of the QGP.

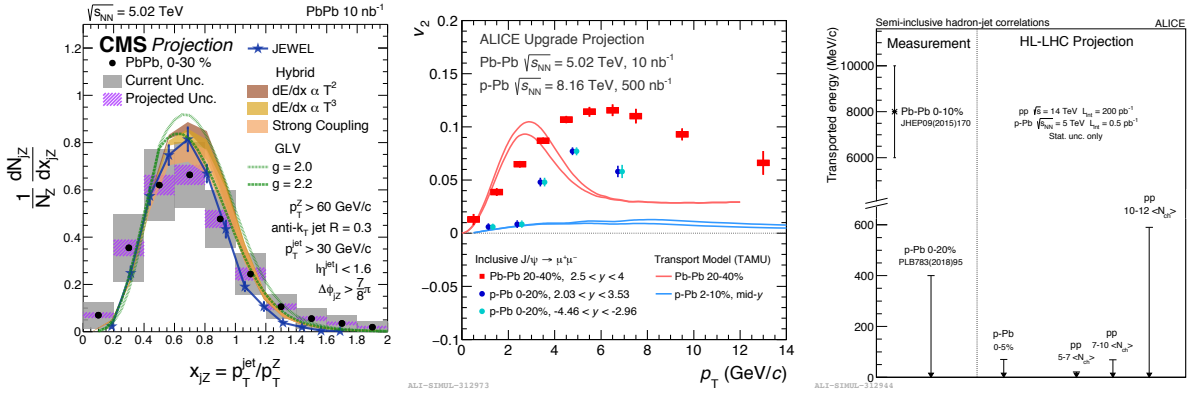

Figure 11. Z–jet momentum imbalance in Pb–Pb (CMS); J/ψ elliptic flow in p–Pb and Pb–Pb (ALICE); limit on jet momentum shift from hadron–jet recoil in Pb–Pb and in high-multiplicity pp and p–Pb collisions (ALICE). From Ref. [5].